Journal of Alloys and Compounds 509 (2011) 7632–7638

Contents lists available at ScienceDirect

Journal of Alloys and Compounds

journal homepage: www.elsevier.com/locate/jallcom

Polyethyleneimine surfactant effect on the formation of nano-sized $BaTiO_3$ powder via a solid state reaction☆

Hsing-I. Hsiang*, Yu-Lun Chang, Jang-Sen Fang, Fu-Su Yen

Particulate Materials Research Center, Department of Resources Engineering, National Cheng Kung University, 70101 Tainan, Taiwan, ROC

ARTICLE INFO

Article history:
Received 16 March 2011
Accepted 21 April 2011
Available online 28 April 2011

Keywords:
$BaTiO_3$
Solid state reaction
Mechanism
Polyethyleneimine

ABSTRACT

Barium titanate powder is widely used in multilayer ceramic capacitors (MLCC) because of its' superior ferroelectric and dielectric properties. Presently, barium titanate powder is mass-produced using a conventional solid state reaction. However, the conflicting literature reports clearly show that the solid state reaction mechanism is not well understood. Synthesizing nano-sized barium titanate powders with less agglomeration using a solid state reaction method at a low calcination temperature has become a hot research topic. This study examines the effect of polyethyleneimine (PEI) surfactant addition on $BaTiO_3$ formation in a solid sate reaction. XRD, DTA and TEM are used in this investigation. The results indicate that PEI addition can promote $BaCO_3$ and TiO_2 mixing homogeneity, which enhances the interfacial reaction between $BaCO_3$ and TiO_2. $BaTiO_3$ formation can be obtained through the interfacial reaction between $BaCO_3$ and TiO_2 at the intimate contact between the reactants and Ti^{+4} ion diffusion along the surfaces or grain boundaries of $BaTiO_3$ powders, thereby obtaining a single phase $BaTiO_3$ powder when calcining at low temperatures for a long period.

1. Introduction

Barium titanate powder is widely used in the multilayer ceramic capacitor (MLCC) due to its' superior ferroelectric and dielectric properties. In recent years, MLCC has developed toward smaller size and higher capacity. Thinner (below 1 μm) green sheets are therefore required. High purity, nano-sized barium titanate powders have progressed to meet the above requirements. The synthesis methods for barium titanate powders can be broadly divided into: solid state reaction, liquid phase reaction and gas phase reaction. High purity, nano-sized $BaTiO_3$ powders are easily obtained using a liquid phase reaction, such as sol–gel, oxalate precipitation and hydrothermal methods. However, the high manufacturing costs and low productivity do not meet the mass production demand. The development rate of $BaTiO_3$ powder synthesis using a gas phase reaction is slower and still in the laboratory stage.

Traditionally, $BaTiO_3$ powder has been synthesized using a solid-state reaction between $BaCO_3$ and TiO_2 at high temperatures (above 1200 °C). However, a solid-state reaction occurring at higher temperatures easily leads to coarsening and agglomeration. Recently, a few researchers succeeded in preparing nano-sized $BaTiO_3$ powders using a solid state reaction below 1000 °C [1–13]. Therefore, the synthesis of nano-sized $BaTiO_3$ powder using a solid state reaction has becomes the research focus because of the lower cost, simpler process and higher productivity. Many researches [14–16] investigated the synthesis of $BaTiO_3$ using a solid state reaction between $BaCO_3$ and TiO_2 and reported that the formation mechanism can be explained by multistep reactions as follows: At the initial stage, $BaTiO_3$ is formed at the contact points between $BaCO_3$ and TiO_2. Subsequently, the formation of Ba_2TiO_4 occurs at the interface between $BaTiO_3$ and $BaCO_3$. Finally, the Ba_2TiO_4 reacts with TiO_2 to form single phase $BaTiO_3$ at the terminal stage. Therefore, $BaTiO_3$ formation is dominated by Ba^{+2} diffusion throughout the perovskite layer. The size and shape of the final $BaTiO_3$ is determined by the morphology of the starting TiO_2. However, Buscaglia et al. [1] prepared $BaTiO_3$ from TiO_2 using different sized $BaCO_3$ powders using a solid state reaction. They reported that the formation of $BaTiO_3$ can be facilitated and the intermediate phase, Ba_2TiO_4, can be suppressed using a $BaCO_3$ powder with a smaller particle size as the raw material. They also investigated the isothermal kinetic behaviors of the solid state reaction at different calcination temperatures and observed that the kinetic data is reasonably comparable to the diminishing-core reaction described by Valensi-Cater equation at 700 °C, but the data at higher temperatures, as 800 °C, cannot be satisfactorily described using any diminishing-core models. This is attributed to the complexity of the reaction mechanism which cannot be reduced to a simple case of phase-boundary-controlled growth or diffusion controlled growth

☆ Supported by the National Science Council of the Republic of China under Contract NSC97-2221-E-006-010.

* Corresponding author. Tel.: +886 6 2757575x62821; fax: +886 6 2380421.
E-mail address: hsingi@mail.ncku.edu.tw (H.-I. Hsiang).

0925-8388/$ – see front matter © 2011 Elsevier B.V. All rights reserved.
doi:10.1016/j.jallcom.2011.04.116

Table 1
Properties of raw materials.

Starting materials	BET (m^2/g)	Impurity						
		Fe (ppm)	Cl (ppm)	$CaCO_3$ (ppm)	$SrCO_3$ (ppm)	Na_2CO_3 (ppm)	Al (ppm)	Loss on ignition (%)
TiO_2	11	<10	250	–	–	–	<10	–
$BaCO_3$ (PBT)	3.02	0.1	863	20	10	2	–	1.2
$BaCO_3$ (PB3T)	30.6	0.3	<25	40	200	17	–	2.42

over the entire temperature range. The conflicting literature reports and inadequate support for either mechanism clearly show that the solid state reaction mechanism is not well understood.

This study examines the effects of polyethyleneimine (PEI) surfactant addition on $BaTiO_3$ formation using a solid sate reaction. X-ray diffractometry (XRD), differential thermogravimetry and thermogravimetry (DTA/TG) and transmission electron microscopy (TEM) are used to characterize this reaction. A solid state reaction mechanism is proposed that helps to obtain nano-sized $BaTiO_3$ powder at lower calcination temperatures.

2. Experimental

The starting powders used in this study and their properties are shown in Table 1.

2.1. Materials preparation

Five gram $BaCO_3$ powders with 100 ml of added (0.5, 1, 1.5 mg/l) PEI solutions at different concentrations were adjusted by adding NH_4OH until pH = 10 and magnetically stirred in polyethylene bottles for 18 h. An equimolar TiO_2 powder was then added and adjusted with HCl until pH = 8.4. The slurry was then magnetically stirred for 12 h and dried at 120 °C for 12 h.

2.2. Thermal treatment

To observe the phase transformation effect on the $BaCO_3$ and TiO_2 reaction the thermal treatment was carried out at 600–1000 °C using different soak times with a heating rate of 10 °C/min. All thermal treatments were conducted in air and under furnace cooling.

2.3. Characterization

(A) X-ray diffractometry: The crystalline phase identification was determined using X-ray diffractometry (Siemens, D5000, Karlsruhe, Germany) with Cu-K_α radiation. The XRD scanning conditions were set at 0.04° per step and each step for 1 s.
(B) Zeta potentiometer: Electrophoretic measurements of the starting materials under different pH values were performed on a zeta potentiometer (Malvern, Zetasizer, Nano ZS, Worcestershire, England).
(C) TEM/EDS analysis: The TEM (Jeol, JEM-3010, Tokyo, Japan) was used to observe the specimen size and morphology. The diffraction patterns of the crystalline species were also obtained using TEM with a camera constant of 80 cm. Semi-quantitative determination of the element content was detected using EDS (Noran, Voyager 1000, Waltham, MA) attached to the TEM.
(D) DTA/TG analysis: The DTA/TG analysis was performed using a thermal analysis instrument (Netzsch STA, 409 PC, Burlington, MA) under 40 ml/min air flow rate. The thermal treatment condition was conducted at a heating rate of 10 °C/min.

3. Results and discussion

3.1. Reaction mechanism of the $BaCO_3$–TiO_2 mixtures without PEI surfactant addition

Fig. 1 shows DTA/TG curves of the $BaCO_3$ (PBT) and TiO_2 mixture. A broad endothermic peaks from around 570 °C to 1070 °C, corresponding to a multiple step weight loss in the same temperature range, can be ascribed to the decarboxylation of $BaCO_3$ [2]. In addition, there is a small endothermic peak around 800 °C, which is attributed to the phase transformation of $BaCO_3$ from the orthorhombic into the hexagonal phase [17].

Based on Ando's report [2], the thermogravimetric weight loss analysis of the $BaCO_3$ and TiO_2 mixture can be separated into two stages. The first stage is related to the contact area between $BaCO_3$ and TiO_2. An increase in the numbers of reactant contact points can enhance this reaction stage. The second reaction stage is attributed mainly to the remaining $BaCO_3$ and TiO_2. A similar mechanism was also proposed by Buscaglia et al. [1]. They reported that the first step in the reaction is dominated by $BaTiO_3$ nucleation and growth at the TiO_2–$BaCO_3$ contact points. $BaCO_3$ surface diffusion is probably the prevailing mass transport mechanism responsible for the rapid formation of $BaTiO_3$ in this stage. The second reaction stage takes place when the residual TiO_2 is completely covered by the product phase. In this stage, the reaction can only proceed by the slower lattice diffusion.

In our DTG results, the $BaCO_3$ and TiO_2 mixture (Fig. 2a) has roughly two stages of weight loss similar to the previous literature results. The first stage, which shows a very small amount of reaction and occurs at around 570 °C, can be reasonably attributed

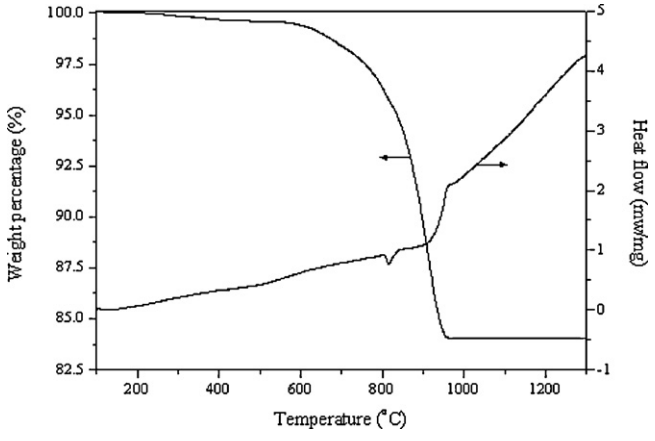

Fig. 1. DTA/TG curves of the $BaCO_3$ and TiO_2 mixture in air with heating rate of 10 °C/min.

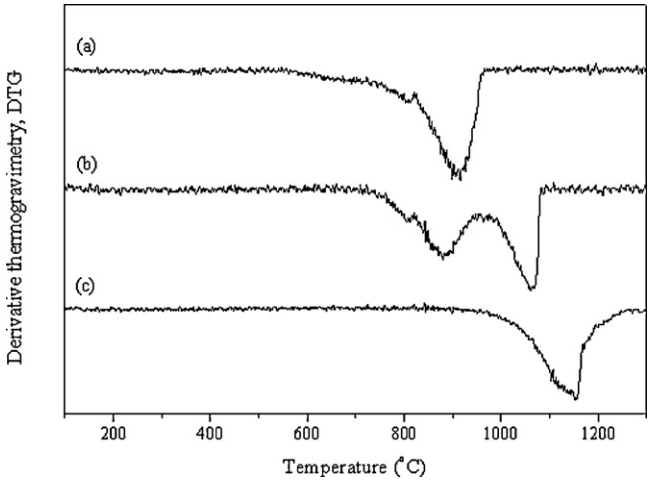

Fig. 2. DTG curves of the mixtures in air with heating rate of 10 °C/min, (a) $BaCO_3$ and TiO_2, (b) $BaCO_3$ and $BaTiO_3$, and (c) $BaCO_3$.

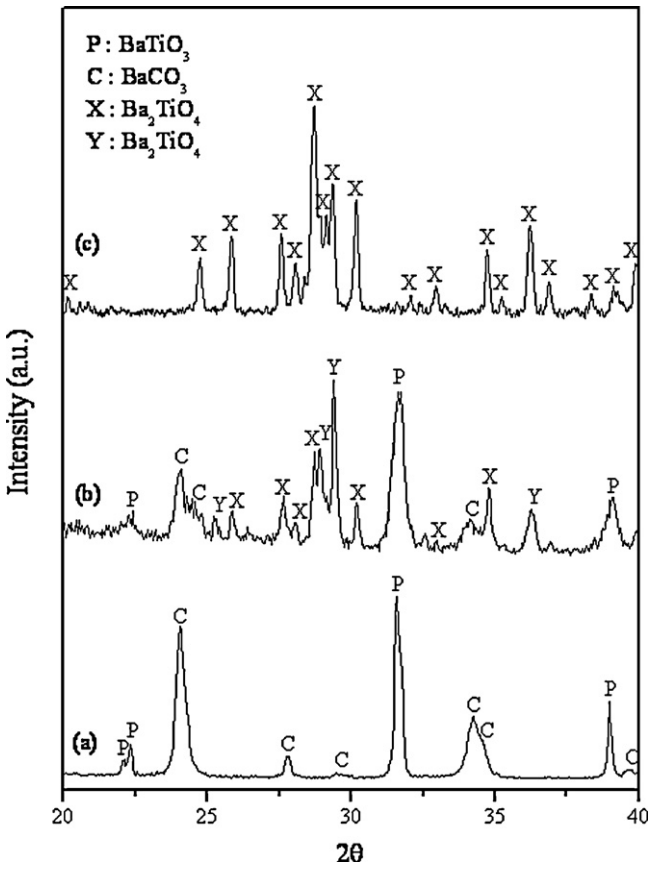

Fig. 3. XRD patterns of the $BaCO_3$ and $BaTiO_3$ mixtures calcined at different temperatures, (a) before calcination, (b) 900 °C, 1 h, and 1100 °C, 1 h.

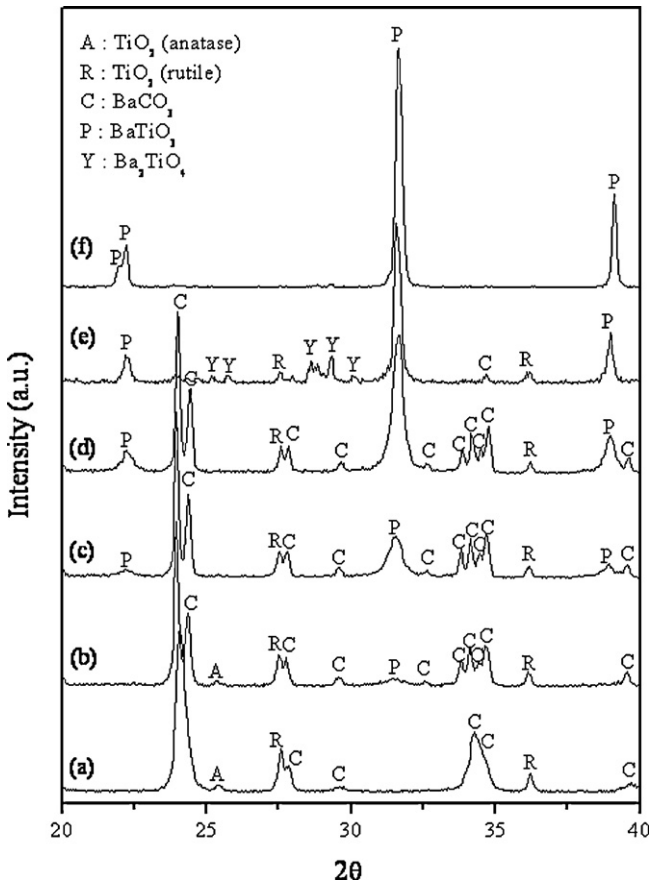

Fig. 4. XRD patterns of the $BaCO_3$ and TiO_2 mixtures calcined at different temperatures, (a) before calcination, (b) 650 °C, 1 h, (c) 720 °C, 1 h, (d) 720 °C, 4 h, (e) 850 °C, 4 h, and (f) 1100 °C, 4 h.

to the directly chemical reaction between $BaCO_3$ and TiO_2 at the contact points [1,2] (Eq. (1)). The second reaction takes place at a temperature around 720–980 °C, with a discontinuous change along the curve at around 800 °C. These features correspond exactly to the first stage of weight loss (720–980 °C) in the reaction between $BaCO_3$ and $BaTiO_3$ (Fig. 2b). According to the XRD observation (Fig. 3a and b), the reaction, which begins at 720 °C, can be attributed to the formation of Ba_2TiO_4 resulting from the chemical reaction between $BaCO_3$ and $BaTiO_3$ (Eq. (2)). This is supported by the findings observed by Niepce and Thomas [16] who reported that the formation of Ba_2TiO_4 can be formed via the reaction between $BaCO_3$ and $BaTiO_3$ in air. The discontinuous changes along the curves at around 800 °C are accompanied with rapid weight losses. It may be due to the Hedvall effect resulted from the polymorphic transformation of $BaCO_3$ [18]. The second stage of weight loss in Fig. 2b occurs at a temperature near 980 °C, at which the decomposition of pure $BaCO_3$ (Fig. 2c) begins. Therefore, this reaction stage can be reasonably implied to be the thermal decomposition of $BaCO_3$ (Eq. (3)).

$$BaCO_3 + TiO_2 \rightarrow BaTiO_3 + CO_2 \quad (1)$$

$$BaCO_3 + BaTiO_3 \rightarrow Ba_2TiO_4 + CO_2 \quad (2)$$

$$BaCO_3 \rightarrow BaO + CO_2 \quad (3)$$

As a result, the solid-state reaction between $BaCO_3$ and $BaTiO_3$ can be separated into three reactions. At 720 °C, the reaction between $BaCO_3$ and $BaTiO_3$ takes place to form a part of the Ba_2TiO_4. Next, $BaCO_3$ is thermally decomposed at 980 °C. Finally, the resulting BaO diffuses through the product layer and reacts with the remaining $BaTiO_3$ [15] to develop pure Ba_2TiO_4 (Eq. (4)) (Fig. 3).

$$BaO + BaTiO_3 \rightarrow Ba_2TiO_4 \quad (4)$$

For the solid-state reaction between $BaCO_3$ and TiO_2 to form $BaTiO_3$, the process can be separated into three stages. The first reaction for the formation of $BaTiO_3$ takes place at around 570 °C, which is suggested to be formed directly at the interface between $BaCO_3$ and TiO_2. The second reaction for the formation of Ba_2TiO_4 due to the reaction between $BaCO_3$ and $BaTiO_3$ occurs at around 720 °C. Ba_2TiO_4 is supposed to locate at the interface between $BaCO_3$ and $BaTiO_3$. It proceeds until the weight loss levels off. As the barium carbonate is reacted completely, Ba_2TiO_4 and the remaining TiO_2 are separated by the $BaTiO_3$ product layer. The final reaction to form pure $BaTiO_3$ (Eq. (5)) must be carried out via a complex material transportation at a higher temperature.

$$Ba_2TiO_4 + TiO_2 \rightarrow 2BaTiO_3 \quad (5)$$

Fig. 4 shows the XRD results for $BaCO_3$ and TiO_2 mixtures calcined under different conditions. This indicates that a small amount of $BaTiO_3$ was formed at 650 °C. The formation of $BaTiO_3$ increased drastically at 720 °C, and then it increased with an increase in the holding time. At 720 °C, the intermediate phase, Ba_2TiO_4, was not observed even under longer calcination time for more than 4 h. When the temperature was raised to 850 °C, $BaCO_3$ diminished and the intermediate phase, Ba_2TiO_4, was observed in addition to the $BaTiO_3$. At 1100 °C, the intermediate phase, Ba_2TiO_4, disappeared and pure $BaTiO_3$ was obtained. This result is consistent with the proposed reaction mechanism between $BaCO_3$ and TiO_2 to form $BaTiO_3$. The formation of Ba_2TiO_4 resulting from the

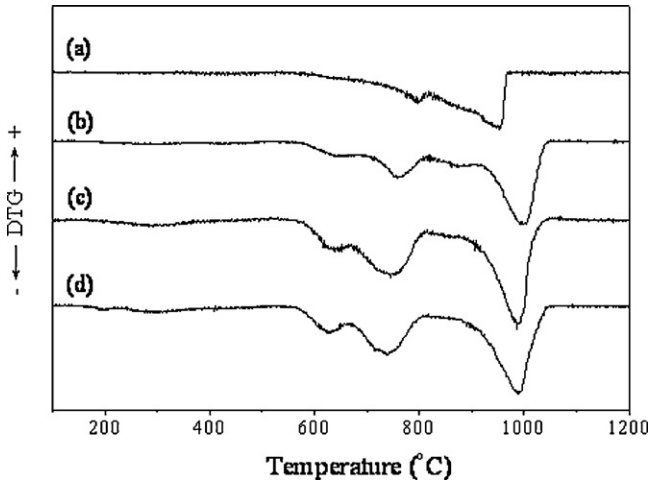

Fig. 5. Variation in derivative thermogravimetry (DTG) curves with different PEI surfactant concentrations (a) 0 mg/ml, (b) 0.5 mg/ml, (c) 1.0 mg/ml, and (d) 1.5 mg/ml for the coarser $BaCO_3$ and TiO_2 mixtures.

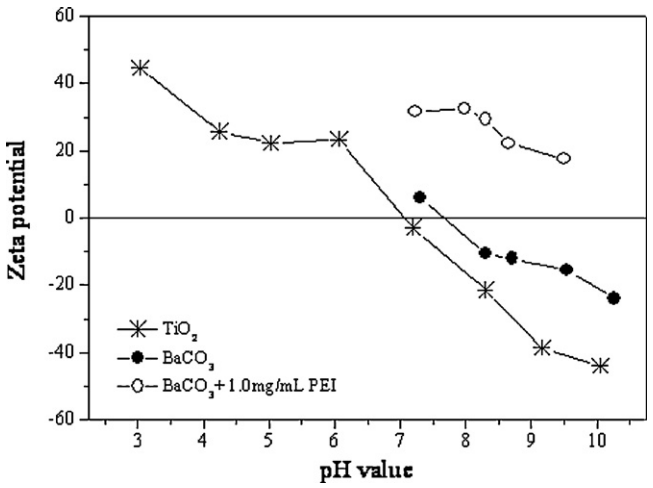

Fig. 6. Zeta potential results as a function of pH for the TiO_2 and $BaCO_3$ powders with and without PEI addition.

reaction between $BaCO_3$ and $BaTiO_3$ should require calcination temperature above 720 °C. As soon as the Ba_2TiO_4 is formed, the reaction between Ba_2TiO_4 and the remaining TiO_2 to form pure $BaTiO_3$ must take place at a higher temperature.

3.2. Reaction mechanism of $BaCO_3$–TiO_2 mixtures with added PEI surfactant

Fig. 5 shows the variation in derivative thermogravimetry (DTG) curves with different PEI surfactant concentrations for the coarser $BaCO_3$ (PBT) and TiO_2 mixtures. It indicates that the DTG curve changes from the original two-stage weight loss into three stages and the weight loss ratio of the first and second stage increased with the increase in PEI concentration. The $BaCO_3$–TiO_2 mixture thermal reaction changed significantly with the addition of a low concentration of PEI surfactant and reached saturation as the PEI concentration increased to 1.0 mg/l. Therefore, the PEI concentration was set at 1.0 mg/l for the next experiment.

3.2.1. First stage

For the sample added with PEI surfactant reaction, the first stage in the DTG curve occurs at about 550–660 °C, which can be attributed to the direct reaction between $BaCO_3$ and TiO_2 as in the previous discussion. Fig. 6 shows the zeta potential results as a function of pH for the TiO_2 and $BaCO_3$ powders with and without PEI addition. For TiO_2 and $BaCO_3$ powders, the isoelectric points are located at pH = 7 and pH = 7.7, respectively. This easily leads to agglomeration making it difficult to mix homogeneously at around pH = 7. However, the zeta potential of $BaCO_3$ powders with PEI addition changed into a highly positive zeta potential value (about 20–30 mV) at pH = 7–9.5. Therefore, TiO_2 and $BaCO_3$ with added PEI powders surfaces are oppositely charged, causing an electrostatic attractive force between them strong enough to form hetero-coagulation at pH = 8.4. This increased the number of TiO_2 and $BaCO_3$ contact points thereby increasing the ratio of the first DTG curve stage as shown in Fig. 1.

3.2.2. Second stage

The second DTG curve stage for the sample with added PEI occurred at the 660–810 °C temperature range, as shown in Fig. 5. The second weight losses for the mixtures with PEI start at about 650 °C, which is below the temperature (720 °C) for the second reaction stage of the mixture without PEI. Fig. 7 shows the XRD patterns for the samples with added PEI calcined at the second stage temperature range, indicating that $BaTiO_3$ formation increases with increasing temperature from 700 to 800 °C with no intermediate phase, Ba_2TiO_4, observed. Therefore, the weight loss mechanism of the samples with added PEI for the second stage is different from that for the sample (720–980 °C) without PEI addition.

Buscaglia et al. [1] reported that the weight loss occurring at the 700–900 °C temperature range was due to $BaCO_3$ decomposition with BaO formation rapidly reacting with TiO_2 leading to $BaTiO_3$. It is well known that the decomposition of $BaCO_3$ is appreciably facilitated with the coexistence of TiO_2. After the first reaction stage, the un-reacted $BaCO_3$ and TiO_2 were separated by $BaTiO_3$ grains, which suppressed the decomposition of un-reacted $BaCO_3$ due to the decomposition temperature of pure $BaCO_3$ in air must be greater than 893 °C [19]. Therefore, at this low temperature range (650–810 °C), the reaction involving a decomposition of $BaCO_3$ into BaO and CO_2, and a subsequent reaction of BaO with TiO_2 are unlikely. Moreover, the intermediate phase, Ba_2TiO_4, resulted from the direct reaction of $BaTiO_3$ and $BaCO_3$ was not observed at this temperature range. Thus the weight loss mechanism at 650–810 °C for the sample with added PEI may be different from the finding observed by Buscaglia et al. [1] and there is other reason to induce the decomposition of $BaCO_3$. The TEM micrographs and diffraction

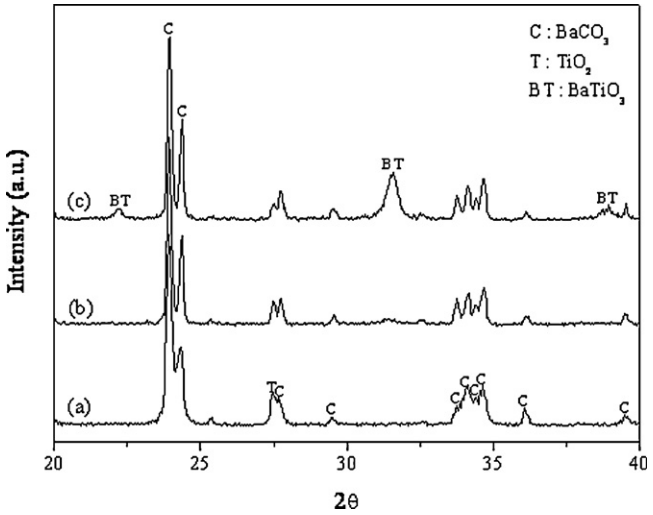

Fig. 7. XRD patterns for the samples with added PEI calcined at the second stage temperature range (a) 600 °C, (b) 700 °C, and (c) 800 °C.

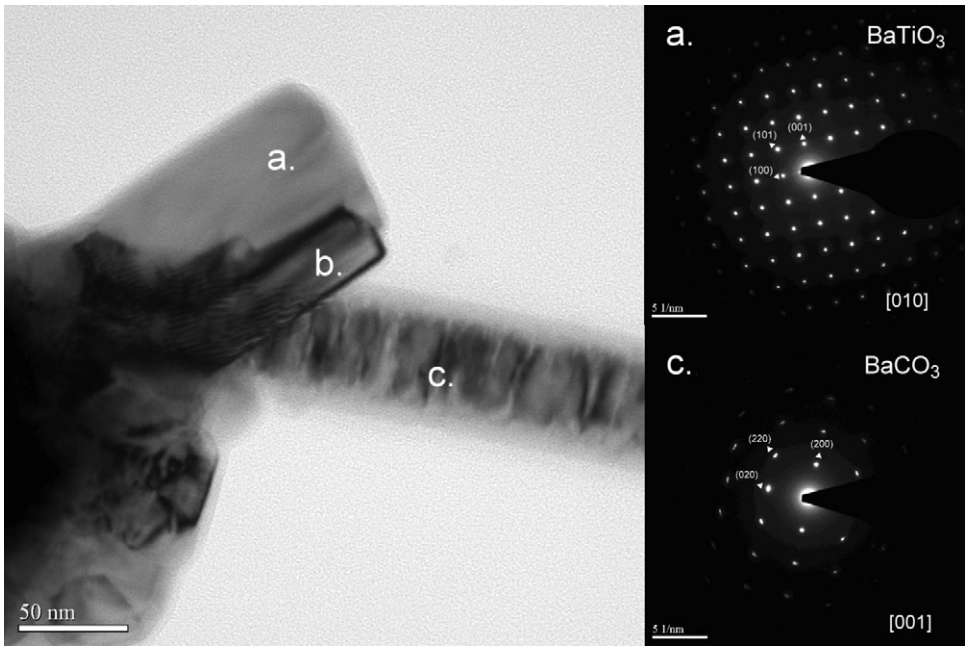

Fig. 8. TEM micrographs and diffraction patterns for the specimen with added PEI calcined at 800 °C for 1 h.

patterns (DP) for the specimen with added PEI calcined at 800 °C for 1 h are shown in Fig. 8. The areas a and c can be identified as $BaTiO_3$ and $BaCO_3$, respectively based on the DP results. According to the EDS results, the Ti–Ba molar ratios for the areas at a, b, and c, are 0.924, 1.05, and 0.147, respectively. Area c is primarily composed of Ba atoms and a small amount of Ti atoms, indicating a small amount of Ti^{+4} ions is supposed to enter the $BaCO_3$ structure. Lotnyk et al. [20] investigated the thermal diffusion of $BaCO_3$ thin film on a TiO_2 single crystal and also observed that the diffusion of Ti^{+4} ions into the $BaCO_3$ matrix in the temperature range of 600–800 °C. The formation of $BaTiO_3$ nanoparticles instead of continuous layers surrounding the TiO_2 particles at the first step of weight loss was reported by Ando et al. [2] and Buscaglia et al. [1]. In this study, the addition of PEI in the mixture is suggested to increase the mixing homogeneity of the reactants that enhances the reaction between $BaCO_3$ and TiO_2 and the formation of $BaTiO_3$ nanoparticles. Then, Ti^{+4} ions from the un-reacted TiO_2 might diffuse through fast diffusion paths, such as grain boundary or surface diffusion into $BaCO_3$ matrix at the second reaction stage. Templeton and Pask [17] investigated the calcination atmosphere effects (air and CO_2) on $BaTiO_3$ formation using $BaCO_3$ and TiO_2 as the starting materials. They observed that in a CO_2 atmosphere, the $BaCO_3$ decomposition temperature increased with Ba_2TiO_4 formation effectively suppressed. Lotnyk et al. [21] investigated the solid state reactions of solid $BaCO_3$ and BaO vapor with rutile substrate and observed that (1) At 800 °C only $BaTiO_3$ was detected in the $BaCO_3$ and TiO_2 reaction; (2) BaO can easily react with TiO_2 to form Ba_2TiO_4 at 700–800 °C; (3) Ti-rich phases, such as $BaTi_4O_9$, $Ba_4Ti_{13}O_{30}$, $Ba_6Ti_{17}O_{40}$, were grown at high reaction temperatures (900–1100 °C). These observations might suggest that the Ba^{+2} ions diffusion into $BaTiO_3$ matrix easily results in the formation of Ba_2TiO_4 at low temperature (700–800 °C) and the reactions due to the diffusion of Ti^{+4} ions into $BaTiO_3$ matrix will not occur until temperature is above 900 °C. The above observations are consistent with our suggestion that the formation of $BaTiO_3$ in the second reaction stage (650–810 °C) for the samples added with PEI might be formed by the diffusion of Ti^{+4} ions into $BaCO_3$ lattice through the $BaTiO_3$ layer and proceeding with direct reaction between $BaCO_3$ and TiO_2.

3.2.3. Third stage

Fig. 9 presents the XRD pattern of the sample added with PEI calcined at 1000 °C, indicating the formation of a significant amount of Ba_2TiO_4. This may be due to the third stage weight loss observed by DTG (910–1060 °C). $BaCO_3$ started to decompose and then Ba^{+2} ions diffused through the $BaTiO_3$ layer according to Eqs. (1)–(4), resulting in the formation of the intermediate phase, Ba_2TiO_4.

In recent years, many researchers reported that ultra fine $BaTiO_3$ powders can be obtained directly, without the formation of the intermediate phase, Ba_2TiO_4, using a solid-state nano-crystalline $BaCO_3$ and TiO_2 reaction and mechanical activation [1–13]. Buscaglia et al. [1] and Ando et al. [2] considered using nano-crystalline $BaCO_3$ and TiO_2 as raw materials and mechanical activation can increase the homogeneity and contact points of the starting mixture, thereby promoting the reaction according to Eq. (1). The Ba^{+2} ions migrate on the $BaTiO_3$ nano-particle surface formed at the first step and diffuse into un-reacted TiO_2, leading

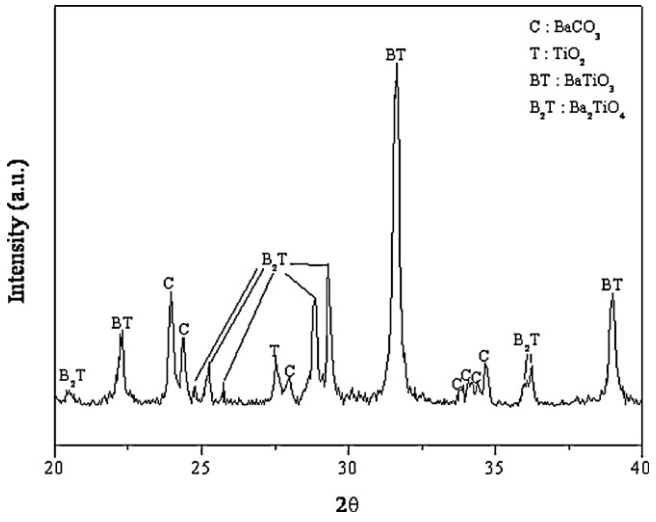

Fig. 9. XRD pattern of the sample added with PEI calcined at 1000 °C.

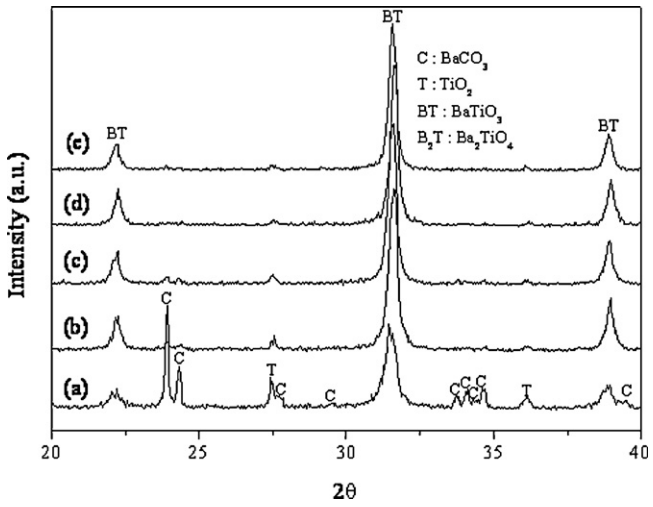

Fig. 10. XRD patterns of the $BaCO_3$–TiO_2 mixtures using small-sized $BaCO_3$ as a raw material with PEI surfactant addition and calcined at 800 °C for different periods (a) 3 min, (b) 1 h, (c) 2 h, (d) 3 h, and (e) 8 h.

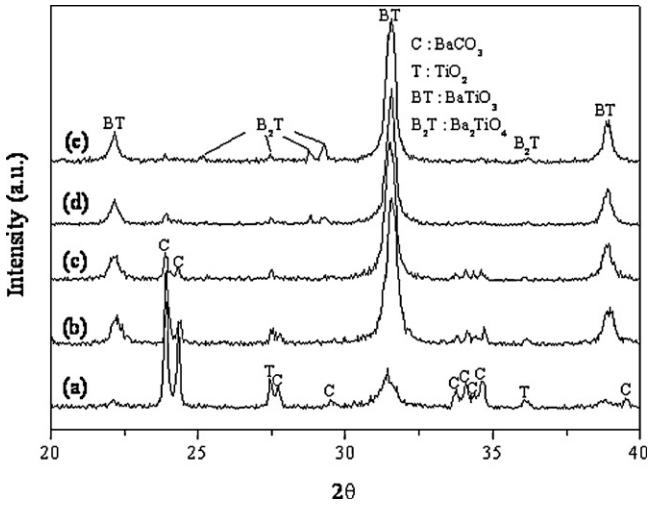

Fig. 11. XRD patterns of the $BaCO_3$–TiO_2 mixtures using small-sized $BaCO_3$ (PB3T) as a raw material without PEI surfactant addition and calcined at 800 °C for different periods (a) 3 min, (b) 1 h, (c) 2 h, (d) 3 h, and (e) 4 h.

to $BaTiO_3$ at below 800 °C. However, at the 600–800 °C temperature range $BaCO_3$ has not yet decomposed, making the probability for Ba^{+2} ion diffusion very low. Moreover, the diffusion of Ba^{+2} ions into $BaTiO_3$ matrix easily results in the formation of Ba_2TiO_4, which was not observed in the mixtures added with PEI and the samples of Buscaglia et al. [1] and Ando et al. [2] calcined at 600–800 °C. Many studies also found that barium titanate formation depended on the particle size of the starting $BaCO_3$. This implies that there seems to be another mechanism evident in controlling the $BaTiO_3$ solid state reaction.

In this study, PEI addition can promote the homogeneous mixing of $BaCO_3$ and TiO_2, and prevents intermediate phase, Ba_2TiO_4, formation. It may be due to the occurrence of Ti^{+4} ions diffusion into the $BaCO_3$ lattice, which promotes $BaTiO_3$ formation before the formation of Ba_2TiO_4 induced by the direct reaction of $BaCO_3$ and $BaTiO_3$ or diffusion of Ba^{+2} across the $BaTiO_3$ layer reaction. Thus, it is expected that homogeneous ultra fine $BaTiO_3$ powders can be obtained by using small-sized $BaCO_3$ to decrease the Ti^{+4} diffusion path and adding PEI surfactant to prevent intermediate phase, Ba_2TiO_4, formation and calcining at the second stage temperature range observed by DTG for a longer period.

3.3. *A single phase $BaTiO_3$ powder obtained by a low-temperature solid state reaction*

Figs. 10 and 11 show the XRD patterns of the $BaCO_3$–TiO_2 mixtures using small-sized $BaCO_3$ (PB3T) as a raw material with and without PEI surfactant addition and calcined at 800 °C for different periods, respectively. Comparison of the samples with and without PEI addition and calcined at 800 °C for 3 min reflects that PEI addition can promote $BaTiO_3$ formation due to the increase in homogeneity and starting mixture contact points. In the case of the sample with added PEI, a nearly single phase was obtained after calcination for 3 h. The *c*/*a* ratio of the resulted $BaTiO_3$ is near 1.0034 and TEM imagine indicates the cubic-like crystallite with size around 50 nm (Fig. 12). However, the intermediate phase, Ba_2TiO_4, was observed after calcining for 3 h and increased with increasing time for the sample without PEI addition. This confirms that improving the mixing homogeneity of the reactants by adding PEI can prevents intermediate phase formation, Ba_2TiO_4, resulting from the direct reaction of $BaCO_3$ and $BaTiO_3$. Therefore, $BaTiO_3$ formation results mainly from the diffusion of Ti^{+4} ions along the $BaTiO_3$ powder surface into the $BaCO_3$ lattice, leading to $BaTiO_3$ for the samples with added PEI calcined at 800 °C for a long period.

The sample using small-sized $BaCO_3$ as the raw material exhibits $BaTiO_3$ formation obtained through the reaction according to Eq. (1) at the intimate contacts between the reactants and the diffusion of Ti^{+4} ions along the surfaces or grain boundaries of $BaTiO_3$ nanoparticles, thereby obtaining a single phase $BaTiO_3$ powder by calcining at the temperature range of the second reaction stage for a long period. In contrast, the sample using coarse $BaCO_3$ powder as the starting material, requires a longer time or higher calcination temperature to complete the reaction through the diffusion of Ti^{+4} ions due to a longer diffusion path caused by the coarser $BaCO_3$ particle size, easily accompanying with the formation of Ba_2TiO_4 resulting from the direct reaction of $BaCO_3$ and $BaTiO_3$.

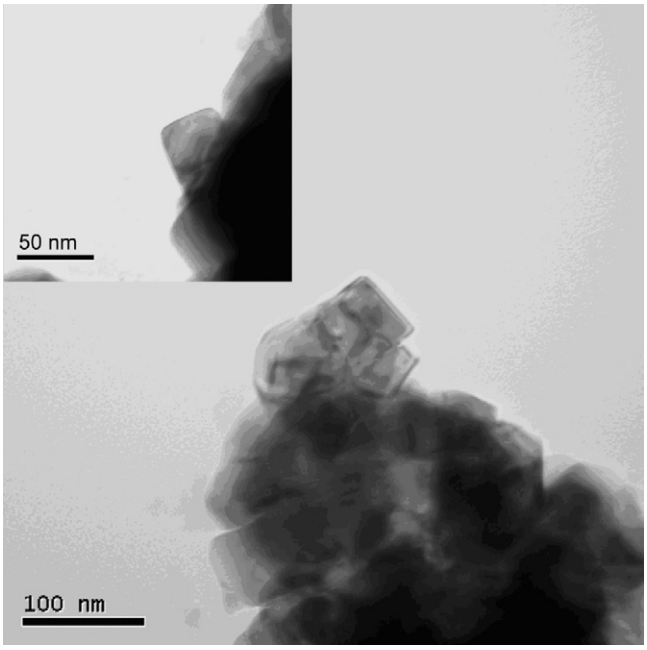

Fig. 12. TEM photograph of the mixture of $BaCO_3$ and TiO_2 using small $BaCO_3$ with 1.0 mg/ml PEI calcined at 800 °C.

4. Conclusions

(1) The solid-state reaction between $BaCO_3$ and TiO_2 to form $BaTiO_3$ is separated into three stages. The first reaction for the formation of $BaTiO_3$ takes place from $BaCO_3$ and TiO_2 at around 570 °C. The second reaction for the formation of Ba_2TiO_4 from $BaCO_3$ and $BaTiO_3$ occurs above 720 °C. This reaction proceeds until the weight loss levels off. As the carbonate is completely reacted, the $BaTiO_3$ product layer may serve as a partition between Ba_2TiO_4 and the remaining TiO_2. Thus, the final reaction to form pure $BaTiO_3$ is suggested carried out via a complex material transportation at a higher temperature.

(2) PEI surfactant addition can change the surface potential of $BaCO_3$ from a negative to a highly positive charge at pH = 7–10, causing strong electrostatic attractive force between $BaCO_3$ and TiO_2 enough to form heterocoagulation at pH = 8.4, which helps to increase the contact points of TiO_2 and $BaCO_3$ at pH = 7–9.5, thereby increasing $BaTiO_3$ formation through the interfacial reaction between $BaCO_3$ and TiO_2.

(3) PEI addition can prevents intermediate phase, Ba_2TiO_4, formation induced by the direct reaction of $BaCO_3$ and $BaTiO_3$.

(4) For samples using small-sized $BaCO_3$ as the raw material, $BaTiO_3$ formation is obtained through the interfacial reaction between $BaCO_3$ and TiO_2 at the intimate contacts between the reactants and the diffusion of Ti^{+4} ions along the surfaces or grain boundaries of $BaTiO_3$ nanoparticles, thereby obtaining a single phase $BaTiO_3$ powder by calcining at low temperatures for a long period.

References

[1] M.T. Buscaglia, M. Bassoli, V. Buscaglia, J. Am. Ceram. Soc. 88 (9) (2005) 2374–2379.
[2] C. Ando, R. Yanagawa, H. Chazono, H. Kishi, M. Senna, J. Mater. Res. 19 (2004) 3592–3599.
[3] D.F.K. Hennings, B.S. Schreinemacher, H. Schreinemacher, J. Am. Ceram. Soc. 84 (12) (2001) 2777–2782.
[4] J. Xue, J. Wang, D. Wan, J. Am. Ceram. Soc. 81 (1) (2000) 232–234.
[5] C. Ando, H. Kishi, H. Oguchi, M. Senna, J. Am. Ceram. Soc. 89 (5) (2006) 1709–1712.
[6] V. Berbenni, A. Marini, G. Bruni, Thermochim. Acta 374 (2001) 151–158.
[7] C. Gomez-Yanez, C. Benitez, H. Balmori-Bamirez, Ceram. Int. 26 (2000) 271–277.
[8] R. Yanagawa, M. Senna, C. Ando, H. Chazono, H. Kishi, J. Am. Ceram. Soc. 90 (3) (2007) 809–814.
[9] S.S. Ryu, S.K. Lee, D.H. Yoon, J. Electroceram. 18 (2007) 243–250.
[10] W. Chaisan, R. Yimnirun, S. Ananta, Ceram. Int. 35 (2009) 173–176.
[11] E. Brzozowski, M.S. Castro, J. Eur. Ceram. Soc. 20 (2000) 2347–2351.
[12] K. Kobayashi, T. Suzuki, Y. Mizuno, Appl. Phys. Exp. 1 (2008) 041602.
[13] M.T. Buscaglia, V. Buscaglia, R. Alessio, Chem. Mater. 19 (2007) 711–718.
[14] A. Beauger, J.C. Mutin, J.C. Niepce, J. Mater. Sci. 18 (1983) 3041–3046.
[15] A. Beauger, J.C. Mutin, J.C. Niepce, J. Mater. Sci. 18 (1983) 3543–3550.
[16] J.C. Niepce, G. Thomas, Solid State Ionics 43 (1990) 69–76.
[17] L.K. Templeton, J.A. Pask, J. Am. Ceram. Soc. 42 (5) (1959) 212–216.
[18] J. Bera, D. Sarkar, J. Electroceram. 11 (2003) 131–137.
[19] S. Kumar, G.L. Messing, W.B. White, J. Am. Ceram. Soc. 76 (3) (1993) 617–624.
[20] A. Lotnyk, S. Senz, D. Hesse, Solid State Ionics 177 (2006) 429–435.
[21] A. Lotnyk, S. Senz, D. Hesse, Acta Mater. 55 (2007) 2671–2681.